

# Vortex Multiplication in Applied Flow: a Precursor to Superfluid Turbulence

A.P. Finne,<sup>1</sup> V.B. Eltsov,<sup>1,2</sup> G. Eska,<sup>3</sup> R. Hänninen,<sup>4</sup> J. Kopu,<sup>1</sup> M. Krusius,<sup>1</sup> E.V. Thuneberg,<sup>5</sup> and M. Tsubota<sup>4</sup>

<sup>1</sup>Low Temperature Laboratory, Helsinki University of Technology, Espoo, Finland

<sup>2</sup>Kapitza Institute for Physical Problems, Moscow, Russia

<sup>3</sup>Physikalisches Institut, Universität Bayreuth, Bayreuth, Germany

<sup>4</sup>Department of Physics, Osaka City University, Osaka, Japan

<sup>5</sup>Department of Physical Sciences, University of Oulu, Oulu, Finland

(Dated: May 26, 2018)

A surface-mediated process is identified in  $^3\text{He-B}$  which generates vortices at roughly constant rate. It precedes a faster form of turbulence where inter-vortex interactions dominate. This precursor becomes observable when vortex loops are introduced in low-velocity rotating flow at sufficiently low mutual friction dissipation at temperatures below  $0.5 T_c$ . Our measurements indicate that the formation of new loops is associated with a single vortex interacting in the applied flow with the sample boundary. Numerical calculations show that the single-vortex instability arises when a helical Kelvin wave expands from a reconnection kink at the wall and then intersects again with the wall.

PACS numbers: 67.40.Vs, 47.37.+q, 98.80.Cq

In superfluid  $^3\text{He-B}$  a hydrodynamic transition takes place below  $0.6 T_c$  from regular (laminar) vortex flow at high temperatures to turbulent flow at low temperatures [1]. The transition occurs as a function of damping in vortex motion, the mutual friction dissipation, which increases roughly exponentially [2] with temperature. If a bundle of vortex loops is injected in applied flow, below  $0.6 T_c$  they interact generating new loops in a rapidly growing tangle of vortices. The onset temperature of this turbulence depends on the number of injected loops. At low enough temperature even a single injected vortex ring leads to turbulence. This is surprising since turbulence is thought to result from the collective interaction of many loops. Also in numerical calculations one ring does not lead to turbulence when placed in uniform applied bulk flow. What is the explanation of this conflict?

Liquid helium flow is generally contained inside solid walls and thus the interaction of the expanding vortex ring with the sample boundary has to be examined. Our measurements indicate that initially the injected ring generates new vortices while interacting with the container wall. This is observed as slow vortex formation which precedes the later more rapid turbulence and has a lower onset temperature. It supplies new vortices so that ultimately rapid turbulence will switch on at some location where the loop density has grown sufficiently.

The existence of a slow precursor, which later escalates to rapid turbulence, is duplicated in numerical simulations. They show that a helical Kelvin wave [3, 4] expands on a single vortex when it becomes aligned sufficiently parallel to the flow. A growing Kelvin wave may then reconnect at the boundary, creating one new vortex as well as sharp kinks. These kinks excite new Kelvin waves [5], starting a self-repeating process of vortex multiplication. We call multiplication a process in which new vortices are formed as a result of the dynamic evolution of existing vortices.

*Experiment:*—We measure with NMR the evolution in the number of vortices when vortex loops are introduced with different techniques in applied flow. Our sample of  $^3\text{He-B}$  is contained in a quartz tube of length  $d = 110$  mm and inner radius  $R = 3$  mm. The flow is created by rotating the sample around its axis with constant angular velocity  $\Omega$ . Initially the sample is vortex-free and the applied flow arises from the difference of the normal and superfluid velocities, the counterflow velocity  $\mathbf{v}_{cf} = \mathbf{v}_n - \mathbf{v}_s$ . If viewed from the laboratory, the normal component is in solid body rotation,  $\mathbf{v}_n = \Omega \times \mathbf{r}$ , while the superfluid component is stationary,  $\mathbf{v}_s = 0$ . The maximum velocity  $v_{cfm} = \Omega R$  is at the cylindrical boundary. Such a state is possible if  $v_{cfm}$  is maintained below a container-dependent critical value [6]. This requirement is here observed so that the growth in vortex number  $N(t)$  monitors vortex multiplication after injection.

In the over-damped regime of vortex motion  $T > 0.6 T_c$ , the injected loops expand to rectilinear lines, conserving their number. In their lowest energy state they form a central cluster where the  $N$  straight lines are packed with an areal density  $n = 2\Omega/\kappa$ . Here  $\kappa = h/2m_3$  is the circulation quantum. Outside the cluster the counterflow increases from zero to  $v_{cfm} = [1 - N/(\pi R^2 n)]\Omega R$  at the cylindrical boundary. Well within the underdamped regime  $T < 0.6 T_c$ , the injection ultimately always leads to rapid turbulence. Its signature is to create close to the equilibrium number of lines,  $N \lesssim \pi R^2 (2\Omega/\kappa)$ .  $N$  can be deduced at the top and bottom of the long sample by measuring the NMR spectra with two independent spectrometers [1]. The technique is based on the strong dependence of the spectrum on  $v_{cf}$ . A calibration can be constructed experimentally or by calculating the order parameter texture and its NMR spectrum numerically [7].

In the onset regime  $T \lesssim 0.6 T_c$ , the evolution after injection depends on the injection method. The highest

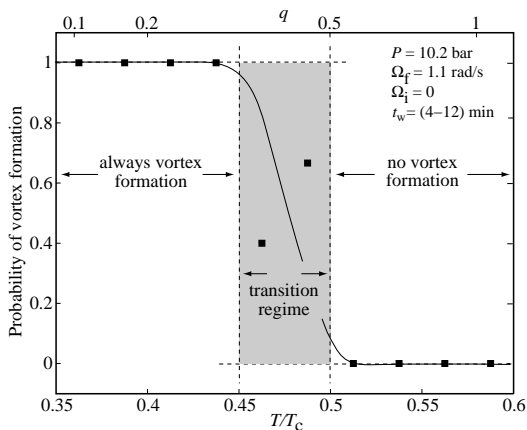


FIG. 1: The probability that vortex multiplication will start from a remnant vortex, when rotation is increased from  $\Omega_i$  to  $\Omega_f$ , plotted vs. temperature (bottom axis) and mutual friction parameter  $q = \alpha/(1 - \alpha')$  (top axis). No vortices are formed above  $0.5 T_c$ . Below  $0.45 T_c$  vortex formation always leads to turbulence. At intermediate temperatures only part of the runs result in vortex formation.

onset for rapid turbulence is measured by making use of the properties of the AB interface between a short section of magnetic-field stabilized  $^3\text{He-A}$  and the remaining  $^3\text{He-B}$  in the long sample [1]. The AB interface undergoes an instability when  $\Omega$  is increased across a well-defined critical value  $\Omega_{\text{cAB}} = 1.2 - 1.6 \text{ rad/s}$  and a bundle of  $\sim 10$  closely spaced loops is tossed on the B-phase side. Measured in this way, the onset is at  $0.59 T_c$  (at 29.0 bar pressure). Its half width of  $0.03 T_c$  we interpret to reflect the variation in the number of injected loops.

The lowest onset is measured by exploiting vortex formation following absorption of a thermal neutron in  $^3\text{He-B}$  [1]. This reaction heats a blob of  $\sim 100 \mu\text{m}$  diameter to the normal state. While the blob rapidly cools back to the ambient temperature a vortex ring with a diameter similar to the blob size is created. The ring starts to inflate and evolve, if  $\Omega$  exceeds a critical value  $\Omega_{\text{cn}} = 1.4 \text{ rad/s}$ . At  $0.59 T_c$  a single ring does not lead to turbulence, but at  $0.45 T_c$  well above 80% of the neutron absorption events at  $\Omega = 1.6 \text{ rad/s}$  develop to turbulence.

This comparison shows that an additional mechanism (requiring a lower value of damping) is needed to start turbulence from a single injected ring than when a bundle of many loops is used. We assume that in the latter case rapid turbulence is switched on immediately at the injection site, while in the former case a precursor mechanism is required. In both cases at  $\Omega \sim 1.4 \text{ rad/s}$  the flow velocity is so high that rapid turbulence follows within seconds and no time is left to monitor a precursor.

These two injection techniques can be accurately controlled, but here the flow velocity cannot be reduced to arbitrary low values. For this two new methods were developed. Conceptually simplest is the case of the remnant

vortex at  $\Omega = 0$  [8]. When rotation is stopped, vortices are rapidly pushed owing to their mutual repulsion to the boundaries for annihilation. Only the annihilation time of the last one or two vortices becomes long below  $0.5 T_c$ , owing to the small dissipation  $\alpha(T)$  and the long sample length. A single straight vortex parallel to the cylinder axis at a distance  $b = \delta R$  from the center survives for a time  $[2\pi R^2/(\alpha\kappa)] [-\ln \delta - \frac{1}{2}(1 - \delta^2)]$ , where the prefactor equals 1 h at  $0.4 T_c$ . In practice the annihilation time can be longer, since the sample and rotation axes cannot be aligned perfectly parallel and the last vortex is not straight. If the time  $t_w$  spent at  $\Omega = 0$  is shorter, then the sample contains a remnant vortex of complex shape.

In Fig. 1 we plot the probability of observing rapid turbulence after the rotation has been increased to  $\Omega_f = 1.1 \text{ rad/s}$  with a remnant vortex in the sample. The abrupt temperature dependence in this figure is characteristic of a transition as a function of rapidly varying mutual friction. No conventional explanation in terms of critical velocities or vortex mill behavior is capable of producing such a steep jump. It is centered at  $0.47 T_c$  while the corresponding value with injection from the AB interface is at  $0.52 T_c$  (at 10.2 bar). In both cases the half widths are  $0.03 T_c$ . We interpret that these two transitions do not overlap and that the case of the remnant vortex in Fig. 1 exemplifies the transition in the single-vortex regime where a precursor is required.

To reveal the precursor, we reduce the applied flow velocity, *ie.* the value of  $\Omega_f$ . The result is shown in Fig. 2, where we plot the growth in the vortex number  $N(t)$  with time. The new feature is the slow approximately linear increase in  $N$  (solid line), before rapid turbulence sets in (dashed lines). At  $\Omega_f = 0.6 \text{ rad/s}$  the slow increase lasts for more than 200 s, generating approximately 1 vortex in 5 s until about 20% of the maximum number of vortices have been created. At larger  $\Omega_f$  the slow increase is shorter in duration, *eg.* at  $\Omega_f = 1 \text{ rad/s}$  rapid turbulence starts already after 30 s. The slow vortex generation at roughly constant rate  $\dot{N}$  we identify as the precursor.

Two further observations about the precursor follow from Fig. 2: (1) Vortex formation proceeds independently in different parts of the sample. At  $\Omega_f = 0.6 \text{ rad/s}$  it takes more than 300 s for a vortex created at one end of the sample to reach the other end [1]. Still, vortex formation at the top and bottom is observed to proceed at roughly the same rate. Thus the precursor is not localized (as would be *eg.* a vortex mill).

(2) In Fig. 2 a second method has been used to introduce vortices in flow, to start from a more controlled initial vortex configuration. The equilibrium vortex state at a low rotation of  $\Omega_i = 0.05 \text{ rad/s}$  is employed as starting point. Here a few vortices in the outer peripheral ring next to the cylinder wall are not rectilinear but connect to the wall (since the sample and rotation axes can only be aligned to within about one degree, see inserts in Fig. 2). To appreciate the influence of these curved

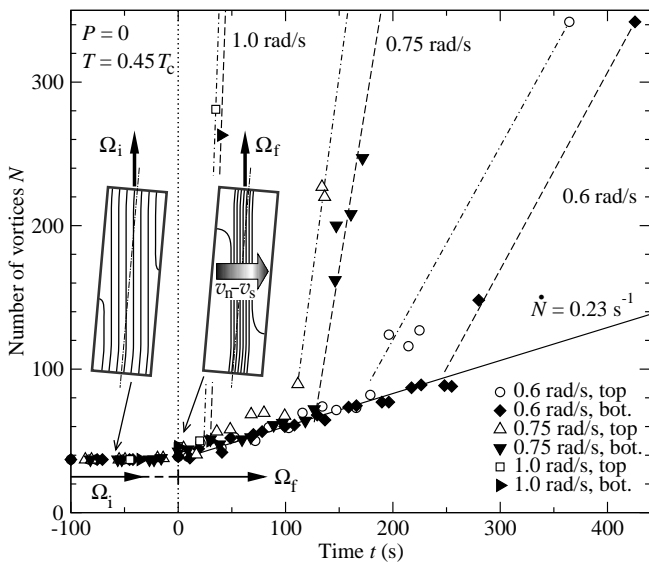


FIG. 2: Vortex formation with a slow precursor which suddenly develops to rapid turbulence. The number of vortices  $N(t)$  is recorded at the top and bottom of the sample. The solid line is the average slow rate  $\dot{N}$  while the dashed lines denote the rapid turbulence. Initially the sample is in the equilibrium vortex state at  $\Omega_i = 0.05$  rad/s with  $N \approx 37$  vortices and a few vortices connecting to the cylinder wall (*left insert*). Rotation is then increased to a new stable value  $\Omega_f$ , which is reached at  $t = 0$ . Three runs with different  $\Omega_f$  are shown. During the ramp to  $\Omega_f$ ,  $N \approx \text{const}$  while the flow builds up and compresses the vortices in a central cluster (*right insert*). The precursor is attributed to an instability of the single vortices, which extend across the counterflow region and end at the cylindrical boundary.

vortices, the experiment was repeated differently.

A cluster with only rectilinear vortices, but with less than the equilibrium number, can be prepared at higher temperatures and can then be cooled to  $T < 0.6 T_c$ . As long as this cluster is separated by a sufficiently wide counterflow annulus from the cylindrical boundary,  $\Omega$  can be increased or decreased without change in  $N$  at any temperature down to our lowest value of  $0.35 T_c$ . If  $\Omega$  is reduced too much, the cluster makes contact with the cylindrical boundary, some outermost vortices become curved, and during a subsequent increase of  $\Omega$ , while  $T < 0.5 T_c$ , the behavior in Fig. 2 is reproduced. Therefore to observe vortex multiplication at  $\Omega_f$ , we conclude that a curved vortex connecting to the cylindrical wall is required. The number of these initially curved vortices increases with  $\Omega_i$  and thus also the rate  $\dot{N}$  increases with  $\Omega_i$ . Nevertheless, the behavior is also observed when  $\Omega_i = 0$  and one starts from a remnant vortex.

At a low value of  $\Omega_f$  a curved vortex which connects to the cylindrical boundary spends a long time expanding axially along the sample. The vortex segment adjacent to the wall moves in the counterflow created by the rotation and reorients partially along the flow owing

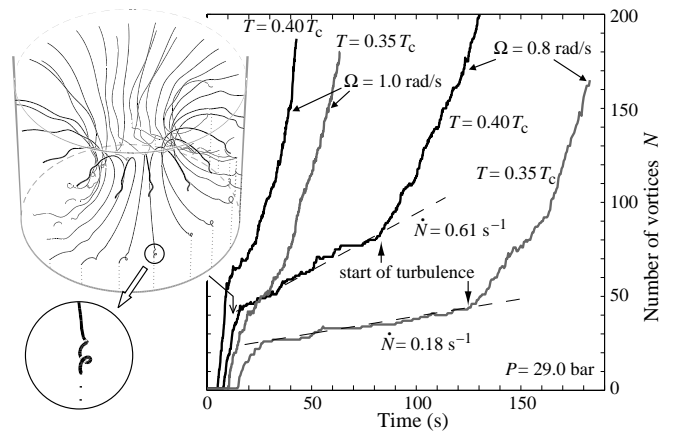


FIG. 3: Simulation of the measurements in Fig. 2. The total number of separate vortices  $N(t)$  vs. time is followed in a cylinder of radius 3 mm and length 10 mm. The calculation is started from a vortex ring of 2 mm radius in the azimuthal plane. The ring is unstable in azimuthal flow and generates via the Kelvin wave instability [3, 4] tens of vortices in a rapid burst, which gives the configuration shown in the *insert*. After this initial burst slow vortex formation at constant average rate  $\dot{N}$  starts. Here each new vortex is produced from Kelvin-waves expanding on an isolated vortex (as shown in the *insert*) which is blown up to ring-like shape and then reconnects at the boundary. The later rapid growth in vortex number is dominated by inter-vortex interactions.

to its self-induced velocity. It is thus expected to become unstable with respect to the formation of Kelvin waves [3, 4]. The expanding waves may then reconnect with the wall and generate new separated loops. This interpretation for the linear precursor in Fig. 2 explains qualitatively its distinct features such as its abrupt temperature dependence or its low threshold velocity. To analyze the precursor in more detail we examine vortex dynamics numerically.

*Simulation.*—The velocity  $\mathbf{v}_L$  of a vortex line element is determined from [3]

$$\mathbf{v}_L = \mathbf{v}_s + \alpha \hat{\mathbf{s}} \times (\mathbf{v}_n - \mathbf{v}_s) - \alpha' \hat{\mathbf{s}} \times [\hat{\mathbf{s}} \times (\mathbf{v}_n - \mathbf{v}_s)]. \quad (1)$$

Here  $\hat{\mathbf{s}}$  is a unit vector parallel to the vortex line element and  $\alpha$  and  $\alpha'$  are the mutual friction parameters measured in Ref. [2]. From the form of this equation we can expect that the solutions for  $\mathbf{v}_L$  can be classified by the parameter  $q = \alpha/(1 - \alpha')$ . We calculate the evolution of the vortex configuration from Eq. (1), with  $\mathbf{v}_s$  obtained from the Biot-Savart law and the boundary conditions derived from an additional solution of the Laplace equation [9, 10]. We apply background flow of  $\mathbf{v}_n$  in different geometries, including rotating flow in a cylinder and flow in a pipe with a uniform or parabolic velocity profile.

We find that at low vortex density new vortices are generated only from expanding Kelvin waves which intersect with a wall. The growth of these waves depends strongly on the orientation of the vortex segment with

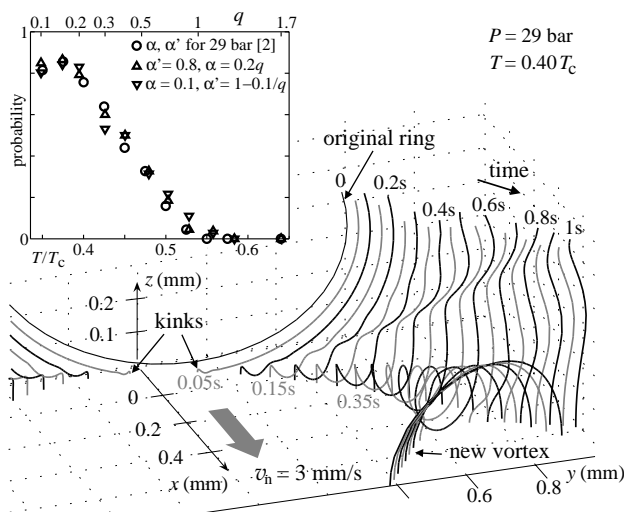


FIG. 4: As a model of the precursor, the collision of a vortex ring with a plane wall (at  $z = 0$ ) is calculated. A ring of 0.5 mm radius is initially above the wall, with the plane of the ring tilted by  $\pi/10$  from the  $x = 0$  plane. In the frame of reference of this figure, uniform flow of the normal component at  $v_n = 3$  mm/s is applied in the  $x$  direction. The different contours show the ring at 0.05 s intervals. The sharp kinks at the wall reconnections induce Kelvin waves on the loop. These are able to grow in the applied flow only on one of the two legs formed in the reconnection (here on the right). The largest wave reconnects with the wall and a new loop is then separated. The conditions for the growth of Kelvin waves are fulfilled in such collisions only in the under-damped temperature regime: The *insert* on the top shows the probability that a new vortex is created when the original ring is initially placed at  $z = 1$  mm with random orientation. This probability depends on the ratio  $q = \alpha/(1 - \alpha')$ , shown on the top axis, rather than on  $\alpha$  or  $\alpha'$  separately.

respect to the flow [4], but it starts from reconnection kinks [5]. It is these sharp kinks which prove to be essential in the simulations for continued generation of new vortices [11]. The kinks are primarily produced when an expanding Kelvin wave hits the wall. In a rotating cylinder this early stage is marked by roughly linear growth in  $N$ , as seen in Fig. 3. Its duration in time is similar to the measurements in Fig. 2 and it also ends in rapid turbulence. The model of this single-vortex instability at the wall is studied in Fig. 4. Here we see the expansion of Kelvin waves from a reconnection kink at the wall and a later reconnection again with the wall, which produces one new loop. The probability of this process has been calculated in the insert. It displays a similar abrupt temperature dependence as measured in Fig. 1.

In numerical calculations self-sustained growth of  $N$  is not started as readily as in our experiment. Uniform flow along a plane wall in Fig. 4 does not support continuous growth. In rotating flow the initial configuration in Fig. 3 had to be specially engineered since experimentally relevant configurations do not necessarily start a continuous process in simulations. Clearly the expla-

nation of this difference is an interesting physical question. Self-sustained vortex multiplication has been previously demonstrated in highly inhomogeneous bulk flow of the normal component [12]. When walls are present we find that the inhomogeneity of the applied flow is not essential to maintain continuous growth in  $N$ . Nevertheless, the flow geometry affects the probability to start self-sustained vortex generation from a single seed loop, which is, for instance, larger in a circular pipe than in a rotating cylinder (at the same value of  $q$ ).

*Conclusions:*—Our results demonstrate that in the under-damped regime of vortex motion intrinsic vortex formation has to be described in an ideal superfluid as a sequence of multiple processes. It starts with the nucleation of the first vortex, is followed by surface-mediated multiplication of more vortex loops, and it finally goes over in rapid turbulence when inter-vortex interactions become possible. These individual steps have been difficult to separate in earlier work. This is because in superfluid  $^4\text{He}$  with strong surface pinning the solid surfaces are covered with a plentiful source of remanent vortices which easily start rapid turbulence when flow is applied. A second reason is that experimentally oscillating flow has been easiest to achieve and there the accumulation of a vortex tangle occurs differently, as was recently reported from measurements with a vibrating grid [13]. We have here focused on the missing link in this chain, the slow surface-mediated precursor to rapid turbulence. If no other mechanism of vortex multiplication intervenes, as is the case in steady flow of  $^3\text{He-B}$  with clean smooth surfaces, then this process will take over.

- 
- [1] A.P. Finne *et al.*, J. Low Temp. Phys. **135**, 479 (2004); *ibid.* **136**, 249 (2004); *ibid.* **138**, 567 (2005).
  - [2] T.D.C. Bevan *et al.*, J. Low Temp. Phys. **109**, 423 (1997); N. Kopnin, Rep. Prog. Phys. **65**, 1633 (2002).
  - [3] R.J. Donnelly, *Quantized Vortices in Helium II*, p. 213 (Cambridge University Press, Cambridge, UK, 1991).
  - [4] R.M. Ostermeier, W.I. Glaberson, J. Low Temp. Phys. **21**, 191 (1975).
  - [5] B.V. Svistunov, Phys. Rev. B **52**, 3647 (1995); D. Kivotides *et al.*, Phys. Rev. Lett. **86**, 3080 (2001).
  - [6] V.M.H. Ruutu *et al.*, J. Low Temp. Phys. **107**, 93 (1997).
  - [7] J. Kopu *et al.*, J. Low Temp. Phys. **120**, 213 (2000).
  - [8] We distinguish between a dynamical *remnant vortex* with finite life time and a *remanent vortex*, preserved by surface pinning indefinitely in metastable state.
  - [9] R. Hänninen *et al.*, J. Low Temp. Phys. **138** (2005).
  - [10] As there is no firm evidence of pinning [6], we use the model of an ideal surface. With surface friction or weak pinning, the single-vortex transition moves to higher  $q$ .
  - [11] The reconnection distance is a fixed parameter. Changing it by an order of magnitude causes no qualitative changes.
  - [12] D.C. Samuels, Phys. Rev. B **47**, 1107 (1993).
  - [13] D.I. Bradley *et al.*, Phys. Rev. Lett. **95**, 035302 (2005).